# Superfluidity of dipolar excitons in doped double-layered hexagonal lattice in a strong magnetic field

Yonatan Abranyos [1], Oleg L. Berman [2], and Godfrey Gumbs[1]

[1]*Department of Physics and Astronomy, Hunter College of the City University of New York, 695 Park Avenue, New York, New York 10065, USA*
[2]*Physics Department, New York City College of Technology of the City University of New York, 300 Jay Street, Brooklyn, New York 11201, USA*

We examine the occurrence of Bose-Einstein condensation and superfluidity of dipolar excitons for a pair of quasi-two-dimensional spatially separated hexagonal $\alpha$-$\mathcal{T}_3$ layers. In the $\alpha$-$\mathcal{T}_3$ model, the $AB$-honeycomb lattice structure is supplemented with C atoms, located at the centers of the hexagonal lattice. We have solved a two-body problem for an electron and a hole for the model Hamiltonian for the $\alpha$-$\mathcal{T}_3$ double layer in a magnetic field. The exciton binding energy is changed due to the magnetic field, and magnetoexcitons are formed as excitons in a magnetic field. The energy dispersion of collective excitations, the spectrum of sound velocity, and the effective magnetic mass of magnetoexcitons are obtained in the integer quantum Hall regime for high magnetic fields. The superfluid density and the temperature of the Kosterlitz-Thouless phase transition are probed as functions of the excitonic density, the magnetic field, and the interlayer separation.

## I. INTRODUCTION

Many-particle systems of dipolar (indirect) excitons, formed by spatially separated electrons and holes, in semiconductor coupled quantum wells (CQWs) in a magnetic field $B$, as well as in the absence of magnetic field, have attracted considerable attention. This interest has been generated in large part by the possibility of Bose-Einstein condensation (BEC) and superfluidity of dipolar excitons, which can be observed as persistent electrical currents in each quantum well and also through coherent optical properties [1–4]. Recent progress in theoretical and experimental studies of the superfluidity of dipolar excitons in CQWs was reviewed in Ref. [5]. Electron-hole superfluids can be realized not only in the BEC regime but also in the BCS-BEC crossover regime [6]. Quantum Monte Carlo simulations obtaining and describing the BCS-BEC crossover physics with electron-hole systems have been performed [7].

Recently, a number of experimental and theoretical studies were dedicated to graphene and the condensation of electron-hole pairs, formed by spatially separated electrons and holes, in a pair of parallel graphene layers. These investigations were reported in Refs. [8–12]. Since the exciton binding energies in novel two-dimensional (2D) semiconductors are quite large, both BEC and superfluidity of dipolar excitons in double layers of transition-metal dichalcogenides (TMDCs) [13–17] and phosphorene [18,19] have been discussed. Possible BEC in a long-lived dark spin state of 2D dipolar excitons was demonstrated for GaAs/AlGaAs semiconductor coupled quantum wells at temperature $T = 1.5$ K with the exciton critical concentration $n_c = 3 - 4 \times 10^{10}$ cm$^{-2}$ [20]. Measurements reveal BEC of dipolar excitons in monolayers of the semiconductors tungsten diselenide and molybdenum diselenide, separated by sheets of the 2D electrical insulator hexagonal boron nitride, at exciton densities of about $10^{12}$ cm$^{-2}$

at temperatures up to 100 K [21]. In high magnetic fields, 2D excitons, referred to as *magnetoexcitons*, exist in a much wider temperature range since the magnetoexciton binding energies increase as the magnetic field is increased [22–28]. Magnetoexcitons in monolayer TMDCs have been studied in Ref. [29].

Lately, there has been growing interest in the electronic properties of the $\alpha$-$\mathcal{T}_3$ lattice for its surprising fundamental physical phenomena as well as its promising applications in solid-state devices [30–43]. For a review of artificial flat-band systems, see Ref. [44]. Raoux *et al.* [30] proposed that an $\alpha$-$\mathcal{T}_3$ lattice could be assembled from cold fermionic atoms confined to an optical lattice by means of three pairs of laser beams for the optical dice lattice ($\alpha = 1$) [45]. A model of this structure shown schematically in Fig. 1 consists of an $AB$-honeycomb lattice (the rim) like that in graphene which is combined with $C$ atoms at the center/hub of each hexagon. A parameter $\alpha$ is then introduced to represent the ratio of the hopping integral between the hub and the rim to that around the rim of the hexagonal lattice. By dephasing one of the three pairs of laser beams, one could possibly vary the parameter, $0 < \alpha = \tan \phi < 1$.

We consider a pair of parallel $\alpha$-$\mathcal{T}_3$ layers separated by an insulating slab [e.g., SiO$_2$ or hexagonal boron nitride ($h$-BN)] in a strong perpendicular magnetic field. The equilibrium system of local pairs of electrons and holes, spatially separated on these parallel $\alpha$-$\mathcal{T}_3$ layers, correspondingly can be created by varying the chemical potential using a bias voltage between the two $\alpha$-$\mathcal{T}_3$ layers or between two gates located near the respective $\alpha$-$\mathcal{T}_3$ 2D sheets [for simplicity, because we consider the BEC regime, we also call these equilibrium local electron-hole ($e$-h) pairs dipolar magnetoexcitons]. In case 1 a dipolar magnetoexciton is formed by an electron in Landau level 1 and a hole in Landau level $-1$. In this case, a dipolar magnetoexciton is formed by the bound state of an
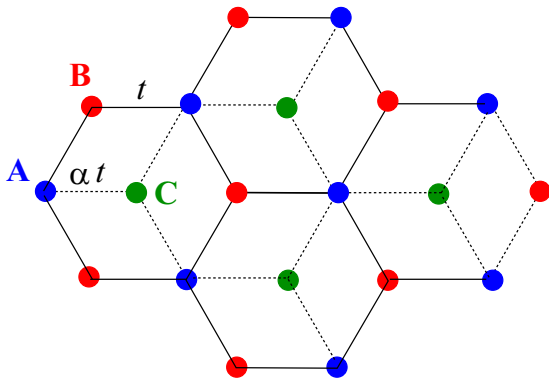
FIG. 1. The $\alpha$-$\mathcal{T}_3$ lattice. Hopping between sites $A$ and $B$, which form a honeycomb lattice identical to graphene, takes place with hopping parameter amplitude $t$. Sites labeled $C$, located at the centers of the hexagons, are coupled only to $A$ sites with variable hopping amplitude $\alpha t$.

electron in the lowest Landau level above the Fermi level and a hole in the highest Landau level below the Fermi level. We choose to consider the lowest-energy state since the energy required to create a magnetoexciton in this state is within the range of energies which are possible to achieve experimentally. Additionally, magnetoexcitons associated with higher Landau levels can eventually transform to magnetoexcitons at lower Landau levels emitting photons. Dipolar magnetoexcitons with spatially separated electrons and holes can also be created by laser pumping and by applying a perpendicular electric field, as done for CQWs [2–4]. In case 2, a dipolar magnetoexciton is formed by an electron in Landau level 1 and a hole in Landau level 0. We assume that the system is in a quasiequilibrium state. We investigate the collective properties and propose the occurrence of superfluidity of dipolar excitons in $\alpha$-$\mathcal{T}_3$ double layers in high magnetic field for both cases 1 and 2. We assume that the dilute system of magnetoexcitons forms a weakly interacting Bose gas.

Our decision to investigate dipolar magnetoexcitons in a double layer versus direct magnetoexcitons in a monolayer was driven by the fact that the $e$-$h$ recombination due to tunneling of electrons and holes between monolayers in a double layer is suppressed by the dielectric barrier, which is placed between two monolayers [9]. Therefore, the dipolar magnetoexcitons, formed by electrons and holes, located in two separate $\alpha$-$\mathcal{T}_3$ layers, have a longer lifetime than direct

magnetoexcitons in a single $\alpha$-$\mathcal{T}_3$ layer. Moreover, due to the interlayer separation $D$, dipolar magnetoexcitons in both the ground and excited states have nonzero electrical dipole moments. The dipole moments of the dipolar magnetoexciton produce a long-range dipole-dipole repulsion between magnetoexcitons, which leads to larger sound velocity and, consequently, higher critical temperature for superfluidity of dipolar magnetoexcitons in a double layer compared with direct excitons in a monolayer with the same magnetoexciton densities.

The rest of the paper is organized in the following way. In Sec. II, the model for electrons in an $\alpha$-$\mathcal{T}_3$ monolayer in a perpendicular magnetic field is reviewed to establish our notation. In Sec. III, the two-body problem for an electron and a hole, spatially separated in two parallel $\alpha$-$\mathcal{T}_3$ monolayers in a perpendicular magnetic field, is formulated, and the corresponding eigenenergies and wave functions are derived. In Sec. IV, the effective masses and binding energies for isolated dipolar magnetoexcitons in the $\alpha$-$\mathcal{T}_3$ double layer are obtained. The collective properties and superfluidity of the weakly interacting Bose gas of dipolar magnetoexcitons in the $\alpha$-$\mathcal{T}_3$ double layer are investigated in Sec. V. Our conclusions are presented in Sec. VI.

## II. $\alpha$-$\mathcal{T}_3$ MODEL IN A MAGNETIC FIELD

The tight-binding Hamiltonian single $\alpha$-$\mathcal{T}_3$ layer is obtained by including additional hopping terms in a single-layer graphene Hamiltonian. The additional terms describe the hopping between the central $C$ atom to the appropriate nearest-neighbor $C$ atoms and $A$ atoms:

$$\hat{H} = \left[ -t \sum_{\langle i,j \rangle \sigma} a_{i\sigma}^\dagger b_{j\sigma} - \alpha t \sum_{\langle i,j \rangle \sigma} a_{i\sigma}^\dagger c_{j\sigma} \right] + \text{H.c.} \quad (1)$$

The first term describes the graphene Hamiltonian, and the term $-\alpha t \sum_{\langle i,j \rangle \sigma} a_{i\sigma}^\dagger c_{j\sigma} + \text{H.c.}$ describes the hopping to the central $C$ atoms corresponding to the $\alpha$-$\mathcal{T}_3$ model.

In the low-energy regime the tight-binding Hamiltonian reduces to a linear term in momentum, and we have the Weyl-Dirac system. This could be described by a model Hamiltonian around the $K$ and $K'$ points of the Brillouin zone describing the lower-energy states since we are interested in the excitonic BEC characterized by the macroscopic occupation of the lowest-energy state. In the absence of magnetic field, the Hamiltonian near the $K$ point is given by

$$\hat{H} = \hbar v_F \begin{pmatrix} 0 & (p_x + ip_y)\cos\phi & 0 \\ (p_x - ip_y)\cos\phi & 0 & (p_x + ip_y)\sin\phi \\ 0 & (p_x - ip_y)\sin\phi & 0 \end{pmatrix}, \quad (2)$$

with $v_F$ being the Fermi velocity and the parameter $\alpha = \tan\phi$ describing the strength of the hopping to the central $C$ atoms. In the presence of a magnetic field $\mathbf{B} = B\hat{\mathbf{e}}_z$ parallel to the $z$ axis, we use the Landau gauge $\mathbf{A} = xB\hat{\mathbf{e}}_y$ with minimal coupling $\mathbf{p} \to \mathbf{p} \pm e\mathbf{A}$ for electrons and holes. In addition, we have Zeeman splitting and a term for pseudospin splitting. For now we ignore the Zeeman and pseudospin splitting. With the minimal coupling substitution in the Landau gauge we obtain the Hamiltonian for electrons and holes using the annihilation operators for an electron and a hole as follows:

$$c_\pm = \frac{1}{\sqrt{2\hbar eB}}[p_x + i(p_y \mp exB)], \quad [c_+, c_+^\dagger] = 1, \quad [c_-, c_-^\dagger] = 1, \quad c_+^\dagger c_+ = \hat{n}_+, \quad c_-^\dagger c_- = \hat{n}_-. \quad (3)$$

The Hamiltonians for the $K$ and $K'$ valleys are given in terms of these operators:

$$H_{\text{kin}}^{eK} = \sqrt{2}\frac{\hbar v_F}{r_B}\begin{pmatrix} 0 & c_+\cos\phi & 0 \\ c_+^\dagger\cos\phi & 0 & c_+\sin\phi \\ 0 & c_+^\dagger\sin\phi & 0 \end{pmatrix}, \quad H_{\text{kin}}^{eK'} = \sqrt{2}\frac{\hbar v_F}{r_B}\begin{pmatrix} 0 & c_+^\dagger\cos\phi & 0 \\ c_+\cos\phi & 0 & c_+^\dagger\sin\phi \\ 0 & c_+\sin\phi & 0 \end{pmatrix}. \tag{4}$$

The two independent modes, around $K$ and $K'$, describing the full low-energy Hamiltonian take the form

$$H_{\text{kin}}^{e} = \sqrt{2}\frac{\hbar v_F}{r_B}\begin{pmatrix} 0 & c_+\cos\phi & 0 & 0 & 0 & 0 \\ c_+^\dagger\cos\phi & 0 & c_+\sin\phi & 0 & 0 & 0 \\ 0 & c_+^\dagger\sin\phi & 0 & 0 & 0 & 0 \\ 0 & 0 & 0 & 0 & c_+^\dagger\cos\phi & 0 \\ 0 & 0 & 0 & c_+\cos\phi & 0 & c_+^\dagger\sin\phi \\ 0 & 0 & 0 & 0 & c_+\sin\phi & 0 \end{pmatrix}, \tag{5}$$

and $r_B = \frac{1}{\sqrt{\hbar e B}}$ is a magnetic length scale.

The energy eigenvalues are obtained in a way similar to that for graphene [46], and we obtain for an electron in the $K$ valley

$$\sqrt{2}\frac{\hbar v_F}{r_B}\begin{pmatrix} 0 & c_+\cos\phi & 0 \\ c_+^\dagger\cos\phi & 0 & c_+\sin\phi \\ 0 & c_+^\dagger\sin\phi & 0 \end{pmatrix}\begin{pmatrix} a_n^K(\phi)|n-2\rangle \\ \pm|n-1\rangle \\ b_n^K(\phi)|n\rangle \end{pmatrix} = \varepsilon_{n,s}\begin{pmatrix} a_n^K(\phi)|n-2\rangle \\ \pm|n-1\rangle \\ b_n^K(\phi)|n\rangle \end{pmatrix}, \tag{6}$$

where $|m\rangle$ is a harmonic oscillator wave function. We have a similar equation for the $K'$ valley, giving the energy eigenvalues

$$\varepsilon_{n,s} = \sqrt{2}\,\text{sgn}(n)\frac{\hbar v_F}{r_B}\sqrt{n - \frac{1}{2}(1 + \eta\cos 2\phi)}, \quad \varepsilon_{n,0} = 0 \text{ flat band}, \quad n = 2, 3, \ldots. \tag{7}$$

Here $\eta = \pm 1$, with $\eta = 1$ for the $K$ valley and $\eta = -1$ for the $K'$ valley. The corresponding energy eigenstates for $n = 2, 3, \ldots$ are

$$|\psi_{\pm,n}^K\rangle = \frac{1}{\sqrt{2}}\begin{pmatrix} a_n^K(\phi)|n-2\rangle \\ \pm|n-1\rangle \\ b_n^K(\phi)|n\rangle \end{pmatrix}, \quad |\psi_{\pm,n}^{K'}\rangle = \frac{1}{\sqrt{2}}\begin{pmatrix} a_n^{K'}(\phi)|n\rangle \\ \pm|n-1\rangle \\ b_n^{K'}(\phi)|n-2\rangle \end{pmatrix}. \tag{8}$$

In this notation,

$$a_n^K(\phi) = \sqrt{\frac{(n-1)\cos^2\phi}{n - \cos^2\phi}}, \quad b_n^K(\phi) = \sqrt{\frac{n\sin^2\phi}{n - \cos^2\phi}}, \quad a_n^{K'}(\phi) = -\sqrt{\frac{n\cos^2\phi}{n - \sin^2\phi}}, \quad b_n^{K'}(\phi) = \sqrt{\frac{(n-1)\sin^2\phi}{n - \sin^2\phi}}.$$

For the flat band with $\varepsilon_{n,0} = 0$, the eigenstates are given by,

$$|\psi_{0,n}^K\rangle = \frac{1}{\sqrt{2}}\begin{pmatrix} b_n^K(\phi)|n-2\rangle \\ 0 \\ a_n^K(\phi)|n\rangle \end{pmatrix}, \quad |\psi_{0,n}^{K'}\rangle = \frac{1}{\sqrt{2}}\begin{pmatrix} b_n^{K'}(\phi)|n\rangle \\ 0 \\ a_n^{K'}(\phi)|n-2\rangle \end{pmatrix}.$$

We treat the lowest state $n = 1$ separately. In this case, the eigenvalue problem is

$$H_{\text{kin}}^{eK}|\Psi\rangle = \frac{\hbar v_F}{r_B}\sqrt{2}\begin{pmatrix} 0 & c_+\cos\phi & 0 \\ c_+^\dagger\cos\phi & 0 & c_+\sin\phi \\ 0 & c_+^\dagger\sin\phi & 0 \end{pmatrix}\begin{pmatrix} 0 \\ \alpha|0\rangle \\ \beta|1\rangle \end{pmatrix} = \varepsilon\begin{pmatrix} 0 \\ \alpha|0\rangle \\ \beta|1\rangle \end{pmatrix}. \tag{9}$$

The energy eigenvalues and eigenstates are

$$|\psi_{\pm,1}^K\rangle = \frac{1}{\sqrt{2}}\begin{pmatrix} 0 \\ \pm|0\rangle \\ |1\rangle \end{pmatrix}, \quad \varepsilon_{1,\pm} = \pm\sqrt{2}\frac{\hbar v_F}{r_B}\sin\phi, \tag{10}$$

$$|\psi_{\pm,1}^{K'}\rangle = \frac{1}{\sqrt{2}}\begin{pmatrix} |1\rangle \\ \pm|0\rangle \\ 0 \end{pmatrix}, \quad \varepsilon_{1,\pm} = \pm\sqrt{2}\frac{\hbar v_F}{r_B}\cos\phi. \tag{11}$$
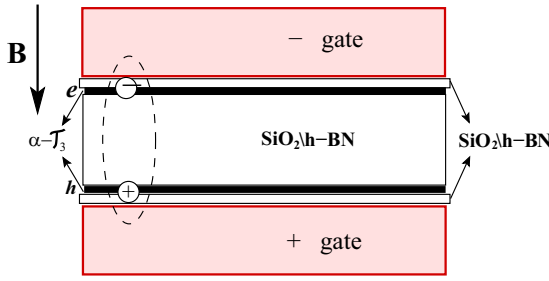
There is no flat-band wave function associated with $n = 1$.

FIG. 2. Schematic illustration of a dipolar magnetoexciton in a pair of $\alpha$-$\mathcal{T}_3$ layers embedded in an insulating material. A uniform perpendicular magnetic field **B** is applied, and negative and positive biases are attached to the layers in the $xy$ plane.

## III. TWO-BODY PROBLEM FOR AN ELECTRON AND A HOLE IN THE $\alpha$-$\mathcal{T}_3$ DOUBLE LAYER IN A PERPENDICULAR MAGNETIC FIELD

We first consider the Hamiltonian for a noninteracting electron-hole pair excluding the Coulomb interaction. We choose the electron-hole state belonging to a single $K$ valley. In general, the magnetoexciton state is a superposition of $K$ and $K'$ valley states. Therefore, we will confine our states to the subspace of $K$ valley states in Eq. (5) (upper right $3 \times 3$ block), i.e.,

$$\hat{H} = H^e_{\text{kin}} \otimes \mathbb{1}_h + \mathbb{1}_e \otimes H^h_{\text{kin}}.$$

In matrix form, we have

$$H^{e-h}_{\text{kin}} = H_{\text{kin}} = \frac{\hbar v_F}{r_B}\sqrt{2}\begin{pmatrix} H^h_{\text{kin}} & c_+ \cos\phi \mathbb{1}_h & 0 \\ c_+^\dagger \cos\phi \mathbb{1}_h & H^h_{\text{kin}} & c_+ \sin\phi \mathbb{1}_h \\ 0 & c_+^\dagger \sin\phi \mathbb{1}_h & H^h_{\text{kin}} \end{pmatrix}. \tag{12}$$

This is a $9 \times 9$ matrix where each entry above is a $3 \times 3$ matrix.

A schematic illustration of a dipolar magnetoexciton, which is a bound state of a spatially separated electron and a hole, located on a pair of $\alpha$-$\mathcal{T}_3$ layers embedded in an insulating material in a perpendicular magnetic field **B**, is depicted in Fig. 2. In the case of noninteracting excitons, the eigenvalues are additive, and we obtain

$$\varepsilon_{n_+,n_-} = \frac{\hbar v_F}{r_B}\sqrt{2}\left(\text{sgn}(n_+)\sqrt{n_+ - \frac{1}{2}(1 + \eta\cos 2\phi)}\,\text{sgn}(n_-)\sqrt{n_+ - \frac{1}{2}(1 - \eta\cos 2\phi)}\right). \tag{13}$$

The general eigenstates are a superposition of product states of the form

$$|\Psi_{n_+,n_-}\rangle = |\psi_{n_+}\rangle \otimes |\psi_{n_-}\rangle, \quad |\Psi\rangle = \sum_{n_+,n_-} a(n_+,n_-)|\Psi_{n_+,n_-}\rangle.$$

We now rewrite the Hamiltonian in the center-of-mass (c.m.) and relative coordinates. The energy of indirect excitons is obtained when a substrate is sandwiched between a double layer of $\alpha$-$\mathcal{T}_3$. We then have the Coulomb term $u(\mathbf{r}_e - \mathbf{r}_h)$ between an electron at $\mathbf{r}_e$ and a hole at $\mathbf{r}_h$. The magnetoexciton Hamiltonian is given by

$$
\begin{aligned}
H &= H^e_{\text{kin}} \otimes \mathbb{1}_h + \mathbb{1}_e \otimes H^h_{\text{kin}} + u(\mathbf{r}_e - \mathbf{r}_h) \otimes \mathbb{1} \\
&= \hbar v_F \begin{pmatrix} 0 & \cos\phi[p_{ex} + i(p_{ey} + eBx_e)] & 0 \\ \cos\phi[p_{ex} - i(p_{ey} + eBx_e)] & 0 & \sin\phi[p_{ex} + i(p_{ey} + eBx_e)] \\ 0 & \sin\phi[p_{ex} - i(p_{ey} + eBx_e)] & 0 \end{pmatrix} \otimes \mathbb{1}_h \\
&\quad + \hbar v_F \mathbb{1}_e \otimes \begin{pmatrix} 0 & \cos\phi[p_{hx} - i(p_{hy} - eBx_h)] & 0 \\ \cos\phi[p_{hx} + i(p_{hy} - eBx_h)] & 0 & \sin\phi[p_{hx} - i(p_{hy} - eBx_h)] \\ 0 & \sin\phi[p_{hx} + i(p_{hy} - eBx_h)] & 0 \end{pmatrix}. \tag{14}
\end{aligned}
$$

We go to the center-of-mass and relative coordinate system as follows:

$$\mathbf{p}_{e/h} = \mathbf{P}/2 \pm \mathbf{p}, \quad \mathbf{r}_{e/h} = \mathbf{R} \pm \mathbf{r}/2.$$

We define the pseudospin-1 operators $S_x(\phi)$ and $S_y(\phi)$ as

$$S_x(\phi) = \begin{pmatrix} 0 & \cos\phi & 0 \\ \cos\phi & 0 & \sin\phi \\ 0 & \sin\phi & 0 \end{pmatrix}, \quad S_y(\phi) = i\begin{pmatrix} 0 & -\cos\phi & 0 \\ \cos\phi & 0 & -\sin\phi \\ 0 & \sin\phi & 0 \end{pmatrix}.$$

The total Hamiltonian is then given by

$$H = \hbar v_F[P_x m_x^+(\phi) + 2p_x m_x^-(\phi) + (P_y - eBx)m_y^-(\phi) + 2p_y m_y^+(\phi) + 2(p_y + eBX)m_y^+(\phi)] + u(\mathbf{r}) \otimes \mathbb{1}.$$

In this notation,

$$m_x^\pm(\phi) = \tfrac{1}{2}[S_x(\phi) \otimes \mathbb{1}_h \pm \mathbb{1}_e \otimes S_x(\phi)],$$
$$m_y^\pm(\phi) = \tfrac{1}{2}[S_y(\phi) \otimes \mathbb{1}_h \pm \mathbb{1}_e \otimes S_y(\phi)].$$

The unitary operator $U = e^{ieBXy}$ transforms the Hamiltonian

$$U^\dagger H U = \hbar v_F[2\mathbf{p} \cdot \mathbf{m}^-(\phi) + (\mathbf{P} - \hat{z} \times \mathbf{r}) \cdot \mathbf{m}^+(\phi)]$$
$$+ u(\mathbf{r}) \otimes \mathbb{1};$$

shifting $\mathbf{r} \to \mathbf{r} - \hat{\mathbf{z}} \times \mathbf{P}$ moves the $\mathbf{P}$ dependence to the potential energy. This gives the same form of two-particle wave function as in [9]. Here are the states and the energies are in the same notation and form as in [9] [see their Eqs. (4) and (6)]. The nine-component wave function is written as follows. Note the symbols have the same definitions as in [9]. We have

$$\Psi(\mathbf{R}, \mathbf{r}) = \exp\left[i\left(\mathbf{P} + \frac{e}{2c}[\mathbf{B} \times \mathbf{r}]\right) \cdot \frac{\mathbf{R}}{\hbar}\right]\tilde{\Phi}(\mathbf{r} - \boldsymbol{\rho}_0). \quad (15)$$

### A. Magnetoexciton states for $n_+$, $n_- = 2, 3, \ldots$

We assume that both electrons and holes are in the $K$ valley, and we first consider $n_+ = 2, 3, \ldots$ and $n_- = 2, 3, \ldots$ states. Therefore, for a magnetoexciton state, we use the tensor product of the above states for the electron-hole wave function. We express the wave function using

$$\Phi_{n_+,n_-}(\mathbf{r}) = (2\pi)^{-1/2}2^{-|m|/2}\frac{\tilde{n}!}{\sqrt{n_+!n_-!}}\frac{1}{r_B}\mathrm{sgn}(m)^m\frac{r^{|m|}}{r_B^{|m|}}$$
$$\times \exp\left[-im\phi - \frac{r^2}{4r_B^2}\right]L_{\tilde{n}}^{|m|}\left(\frac{r^2}{2r_B^2}\right), \quad (16)$$

where $m = |n_+ - n_-|$, $\tilde{n} = \min(n_+, n_-)$, and $L$ are Laguerre polynomials. We have

$$\psi_{n_+}(\mathbf{r}_e) \otimes \psi_{n_-}(\mathbf{r}_h) = \frac{1}{2}\begin{pmatrix} a_{n_+}(\phi)\Phi_{n_+-2}(\mathbf{r}_e) \\ \Phi_{n_+-1}(\mathbf{r}_e) \\ b_{n_+}(\phi)\Phi_{n_+}(\mathbf{r}_e) \end{pmatrix}$$
$$\otimes \begin{pmatrix} a_{n_-}(\phi)\Phi_{n_--2}(\mathbf{r}_h) \\ -\Phi_{n_--1}(\mathbf{r}_h) \\ b_{n_-}(\phi)\Phi_{n_-}(\mathbf{r}_h) \end{pmatrix}. \quad (17)$$

This leads to the following wave function in the c.m. coordinate frame of reference:

$$\tilde{\Phi}_{n_+,n_-}(\mathbf{r}) = \frac{1}{2}\begin{pmatrix} a_{n_+}(\phi)a_{n_-}(\phi)\Phi_{n_+-2,n_--2}(\mathbf{r}) \\ -a_{n_+}(\phi)\Phi_{n_+-2,n_--1}(\mathbf{r}) \\ a_{n_+}(\phi)b_{n_-}(\phi)\Phi_{n_+-2,n_-}(\mathbf{r}) \\ a_{n_-}(\phi)\Phi_{n_+-1,n_--2}(\mathbf{r}) \\ -\Phi_{n_+-1,n_--1}(\mathbf{r}) \\ b_{n_-}(\phi)\Phi_{n_+-1,n_-}(\mathbf{r}) \\ b_{n_+}(\phi)a_{n_-}(\phi)\Phi_{n_+,n_--2}(\mathbf{r}) \\ -b_{n_+}(\phi)\Phi_{n_+,n_--1}(\mathbf{r}) \\ b_{n_+}(\phi)a_{n_-}(\phi)\Phi_{n_+,n_-}(\mathbf{r}) \end{pmatrix}. \quad (18)$$

### B. Landau levels for $n_\pm = 1$

The $n_\pm = 1$ Landau levels are treated separately as described below. We express the eigenvalue problem as

$$H_{\mathrm{kin}}^e|\Psi\rangle = \gamma_B\begin{pmatrix} 0 & c_+\cos\phi & 0 \\ c_+^\dagger\cos\phi & 0 & c_+\sin\phi \\ 0 & c_+^\dagger\sin\phi & 0 \end{pmatrix}\begin{pmatrix} 0 \\ \alpha|0\rangle \\ \beta|1\rangle \end{pmatrix}$$
$$= \varepsilon\begin{pmatrix} 0 \\ \alpha|0\rangle \\ \beta|1\rangle \end{pmatrix}, \quad (19)$$

and we have a similar equation for a hole from which the states are given by

$$\psi_{n_+=1}(\mathbf{r}_e) = \frac{1}{\sqrt{2}}\begin{pmatrix} 0 \\ \pm\Phi_0(\mathbf{r}_e) \\ \Phi_1(\mathbf{r}_e) \end{pmatrix},$$
$$\psi_{n_-=1}(\mathbf{r}_h) = \frac{1}{\sqrt{2}}\begin{pmatrix} 0 \\ \pm\Phi_0(\mathbf{r}_h) \\ \Phi_1(\mathbf{r}_h) \end{pmatrix}. \quad (20)$$

We note that the $n_\pm = 1$ states are independent of the hopping parameter $\phi$.

### C. Magnetoexciton states for $n_+ = 2, 3, \ldots$ and $n_- = 1$

$$\psi_{n_+}(\mathbf{r}_e) \otimes \psi_{n_-}(\mathbf{r}_h) = \frac{1}{2}\begin{pmatrix} a_{n_+}(\phi)\Phi_{n_+-2}(\mathbf{r}_e) \\ \Phi_{n_+-1}(\mathbf{r}_e) \\ b_{n_+}(\phi)\Phi_{n_+}(\mathbf{r}_e) \end{pmatrix}$$
$$\otimes \begin{pmatrix} 0 \\ -\Phi_0(\mathbf{r}_h) \\ \Phi_1(\mathbf{r}_h) \end{pmatrix}. \quad (21)$$

This leads to the following wave function in the c.m. coordinate system:

$$\tilde{\Phi}_{n_+,n_-}(\mathbf{r}) = \frac{1}{2}\begin{pmatrix} 0 \\ -a_{n_+}(\phi)\Phi_{n_+-2,0}(\mathbf{r}) \\ a_{n_+}(\phi)\Phi_{n_+-2,1}(\mathbf{r}) \\ 0 \\ -\Phi_{n_+-1,0}(\mathbf{r}) \\ \Phi_{n_+-1,1}(\mathbf{r}) \\ 0 \\ -b_{n_+}(\phi)\Phi_{n_+,0}(\mathbf{r}) \\ b_{n_+}(\phi)\Phi_{n_+,1}(\mathbf{r}) \end{pmatrix}. \quad (22)$$

### D. Magnetoexciton states for $n_+ = 1$, $n_- = 2, 3, \ldots$

$$\psi_{n_+}(\mathbf{r}_e) \otimes \psi_{n_-}(\mathbf{r}_h) = \frac{1}{2}\begin{pmatrix} 0 \\ \Phi_0(\mathbf{r}_e) \\ \Phi_1(\mathbf{r}_e) \end{pmatrix} \otimes \begin{pmatrix} a_{n_-}(\phi)\Phi_{n_--2}(\mathbf{r}_h) \\ -\Phi_{n_--1}(\mathbf{r}_h) \\ b_{n_-}(\phi)\Phi_{n_-}(\mathbf{r}_h) \end{pmatrix}. \quad (23)$$

This leads to the following wave function in the c.m. coordinate system:

$$
\tilde{\Phi}_{1,n_-}(\mathbf{r}) = \frac{1}{2}
\begin{pmatrix}
0 \\
0 \\
0 \\
a_{n_-}(\phi)\Phi_{0,n_--2}(\mathbf{r}) \\
-\Phi_{0,n_--1}(\mathbf{r}) \\
b_{n_-}(\phi)\Phi_{0,n_-}(\mathbf{r}) \\
a_{n_-}(\phi)\Phi_{1,n_--2}(\mathbf{r}) \\
-\Phi_{1,n_--1}(\mathbf{r}) \\
b_{n_-}(\phi)\Phi_{1,n_-}(\mathbf{r})
\end{pmatrix}.
\tag{24}
$$

### E. Magnetoexciton states for $n_+ = 1, \quad n_- = 1$

We note that for $n = 0$ we have no valence or conduction band states, but there is a flat band described by

$$
\psi_{n_+=1}(\mathbf{r}_e) \otimes \psi_{n_-=1}(\mathbf{r}_h) = \frac{1}{2}
\begin{pmatrix}
0 \\
+\Phi_0(\mathbf{r}_e) \\
\Phi_1(\mathbf{r}_e)
\end{pmatrix}
\otimes
\begin{pmatrix}
0 \\
-\Phi_0(\mathbf{r}_h) \\
\Phi_1(\mathbf{r}_h)
\end{pmatrix},
\tag{25}
$$

which yields the following wave function in the c.m. frame of reference:

$$
\tilde{\Phi}_{n_+=1,n_-=1}(\mathbf{r}) = \frac{1}{2}
\begin{pmatrix}
0 \\
0 \\
0 \\
0 \\
-\Phi_{0,0}(\mathbf{r}) \\
\Phi_{0,1}(\mathbf{r}) \\
0 \\
\Phi_{1,0}(\mathbf{r}) \\
\Phi_{1,1}(\mathbf{r})
\end{pmatrix}.
\tag{26}
$$

### F. Magnetoexciton states for $n_+ = 1, \quad n_- = 0$

For the case when $n = 0$, there is neither a valence nor conduction band, but there is a flat band. We now consider an electron in $n_+ = 1$ and a hole in the flat band with $n_- = 0$. The $n = 0$ state

$$
\psi_{n_-=0}(\mathbf{r}_h) =
\begin{pmatrix}
0 \\
0 \\
\Phi_0(\mathbf{r}_h)
\end{pmatrix}.
\tag{27}
$$

The corresponding exciton state becomes

$$
\psi_{n_+=1}(\mathbf{r}_e) \otimes \psi_{n_-=0}(\mathbf{r}_h) = \frac{1}{\sqrt{2}}
\begin{pmatrix}
0 \\
\Phi_0(\mathbf{r}_e) \\
\Phi_1(\mathbf{r}_e)
\end{pmatrix}
\otimes
\begin{pmatrix}
0 \\
0 \\
\Phi_0(\mathbf{r}_h)
\end{pmatrix}.
\tag{28}
$$

This leads to the following wave function in the c.m. coordinate system:

$$
\tilde{\Phi}_{n_+=1,n_-=0}(\mathbf{r}) = \frac{1}{\sqrt{2}}
\begin{pmatrix}
0 \\
0 \\
0 \\
0 \\
0 \\
\Phi_{0,0}(\mathbf{r}) \\
0 \\
0 \\
\Phi_{1,0}(\mathbf{r})
\end{pmatrix}.
\tag{29}
$$

## IV. ISOLATED DIPOLAR MAGNETOEXCITON

For case 1, we calculate the magnetoexciton energy using the expectation value for an electron in Landau level 1 and a hole in level 1. In high magnetic field, the magnetoexciton is constructed from an electron and a hole in the lowest Landau level with the following nine-component wave function with relative coordinates:

$$
\tilde{\Phi}_{1,1}(\mathbf{r}) =
\begin{pmatrix}
0 \\
0 \\
0 \\
0 \\
-\Phi_{0,0}(\mathbf{r}) \\
\Phi_{0,1}(\mathbf{r}) \\
0 \\
\Phi_{1,0}(\mathbf{r}) \\
\Phi_{1,1}(\mathbf{r})
\end{pmatrix}.
\tag{30}
$$

For case 2, we calculate the magnetoexciton energy using the expectation value for an electron in Landau level 1 and a hole in level 0. We have

$$
\tilde{\Phi}_{1,0}(\mathbf{r}) =
\begin{pmatrix}
0 \\
0 \\
0 \\
0 \\
0 \\
\Phi_{0,0}(\mathbf{r}) \\
0 \\
0 \\
\Phi_{1,0}(\mathbf{r})
\end{pmatrix}.
\tag{31}
$$

The 2D harmonic oscillator eigenfunctions $\Phi_{n_e,n_h}(\mathbf{r})$ are given by [46]

$$
\Phi_{n_e,n_h}(\mathbf{r}) = (2\pi)^{-1/2} 2^{-|m|/2} \frac{\tilde{n}!}{\sqrt{n_1!n_2!}} \frac{1}{r_B} \mathrm{sgn}(m)^m \frac{r^{|m|}}{r_B^{|m|}}
$$

$$
\times \exp\left[-im\phi - \frac{r^2}{4r_B^2}\right] L_{\tilde{n}}^{|m|}\left(\frac{r^2}{2r_B^2}\right),
\tag{32}
$$

where $r_B = \sqrt{\hbar/(eB)}$ is the magnetic length, $L_{\tilde{n}}^{|m|}(x)$ denotes Laguerre polynomials, $m = n_e - n_h$, $\tilde{n} = \min(n_e, n_h)$, and $\mathrm{sgn}(m)^m = 1$ for $m = 0$.

The magnetoexciton energy in high magnetic field can be calculated by employing perturbation theory with respect to the Coulomb electron-hole attraction, analogously to 2D quantum wells with finite electron and hole masses [22]. This approach allows us to derive the spectrum of isolated dipolar magnetoexcitons with spatially separated electrons and holes in the $\alpha$-$\mathcal{T}_3$ double layer. For the $\alpha$-$\mathcal{T}_3$ double layer, this perturbation theory is valid only for relatively large separation $D$ between electron and hole $\alpha$-$\mathcal{T}_3$ double layers and relatively high magnetic fields $B$, i.e., $D \gg r_B$ when $e^2/(\epsilon D) \ll \hbar v_F/r_B$. Here $e^2/(\epsilon D)$ is the characteristic Coulomb electron-hole attraction for the $\alpha$-$\mathcal{T}_3$ double layer, and $\hbar v_F/r_B$ is the energy difference between the first and zeroth Landau levels in $\alpha$-$\mathcal{T}_3$. The operator of electron-hole Coulomb attraction is

$$\hat{V}(r) = -\frac{ke^2}{\epsilon\sqrt{r^2 + D^2}}, \qquad (33)$$

where $k = 9 \times 10^9 \, \mathrm{N} \times \mathrm{m}^2/\mathrm{C}^2$; $\epsilon$ is the dielectric constant of the insulator ($SiO_2$ or $h$-BN), surrounding the electron and hole $\alpha$-$\mathcal{T}_3$ monolayers, forming the double layer; and $D$ is the separation between electron and hole $\alpha$-$\mathcal{T}_3$ monolayers. For the $h$-BN barrier we substitute the dielectric constant $\epsilon = 4.89$, while for the $SiO_2$ barrier we substitute the dielectric constant $\epsilon = 4.5$. For $h$-BN insulating layers, $\epsilon = 4.89$ is the effective dielectric constant, defined as $\epsilon = \sqrt{\varepsilon^\perp}\sqrt{\varepsilon^\parallel}$ [13], where $\varepsilon^\perp = 6.71$ and $\varepsilon^\parallel = 3.56$ are the components of the dielectric tensor for $h$-BN [47]. We will also discuss the case when the $\alpha$-$\mathcal{T}_3$ double layer is surrounded by air.

The magnetoexciton energies $E_{n_+,n_-}(P)$ in first-order perturbation theory are given by

$$E_{n_e,n_h}(P) = E_{n_e,n_h}^{(0)} + \mathcal{E}_{n_e,n_h}(P), \qquad (34)$$

where $E_{n_e,n_h}^{(0)}$ is the unperturbed spectrum and

$$\mathcal{E}_{n_e,n_h}(P) = -\left\langle n_e n_h \mathbf{P} \left| \frac{ke^2}{\epsilon\sqrt{D^2 + r^2}} \right| n_e n_h \mathbf{P} \right\rangle. \qquad (35)$$

Neglecting the transitions between different Landau levels, first-order perturbation with respect to the Coulomb attraction leads to the following result for the energy of magnetoexciton for case 1:

$$\mathcal{E}_{1,1}(P) = -\left\langle 1, 1, \mathbf{P} \left| \frac{ke^2}{\epsilon\sqrt{D^2 + r^2}} \right| 1, 1, \mathbf{P} \right\rangle, \qquad (36)$$

and for case 2,

$$\mathcal{E}_{1,0}(P) = -\left\langle 1, 0, \mathbf{P} \left| \frac{ke^2}{\epsilon\sqrt{D^2 + r^2}} \right| 1, 0, \mathbf{P} \right\rangle. \qquad (37)$$

Denoting the averaging involving the 2D harmonic oscillator eigenfunctions $\Phi_{n_e,n_h}(\mathbf{r})$ in Eq. (32) as $\langle\langle \tilde{n}m\mathbf{P}| \cdots |\tilde{n}m\mathbf{P}\rangle\rangle$ [$\tilde{n}$ and $m$ are defined below Eq. (32)], we obtain the energy of an indirect magnetoexciton created by spatially separated electrons and holes in the lowest Landau level for case 1:

$$\mathcal{E}_{1,1}(P) = \langle 1, 1, \mathbf{P}|\hat{V}(r)|1, 1, \mathbf{P}\rangle$$

$$= \tfrac{1}{4}[\langle\langle 0, 0, \mathbf{P}|\hat{V}(r)|0, 0, \mathbf{P}\rangle\rangle$$
$$+ 2\langle\langle 0, 1, \mathbf{P}|\hat{V}(r)|0, 1, \mathbf{P}\rangle\rangle$$
$$+ \langle\langle 1, 0, \mathbf{P}|\hat{V}(r)|1, 0, \mathbf{P}\rangle\rangle], \qquad (38)$$

and for case 2, we have

$$\mathcal{E}_{1,0}(P) = \langle 1, 0, \mathbf{P}|\hat{V}(r)|1, 0\mathbf{P}\rangle = \tfrac{1}{2}[\langle\langle 0, 0, \mathbf{P}|\hat{V}(r)|0, 0, \mathbf{P}\rangle\rangle$$
$$+ \langle\langle 0, 1, \mathbf{P}|\hat{V}(r)|0, 1, \mathbf{P}\rangle\rangle]. \qquad (39)$$

Substituting for small magnetic momenta $P \ll \hbar/r_B$ and $P \ll \hbar D/r_B^2$, we get the following relations [26]:

$$\langle\langle \tilde{n}m\mathbf{P}|\hat{V}(r)|\tilde{n}m\mathbf{P}\rangle\rangle = \mathcal{E}_{\tilde{n}m}^{(b)} + \frac{P^2}{2M_{\tilde{n}m}(B, D)}. \qquad (40)$$

Making use of this in Eqs. (38) and (39), we obtain the dispersion law of a magnetoexciton for small magnetic momenta in cases 1 and 2, i.e.,

$$\mathcal{E}_{1,1}(P) = \frac{1}{4}\big[\mathcal{E}_{00}^{(b)}(B, D) + 2\mathcal{E}_{01}^{(b)}(B, D) + \mathcal{E}_{10}^{(b)}(B, D)\big]$$

$$+ \frac{1}{4}\left(\frac{1}{M_{00}(B, D)} + \frac{2}{M_{01}(B, D)} + \frac{1}{M_{10}(B, D)}\right)\frac{P^2}{2}$$

$$= -\mathcal{E}_B^{(b)}(D) + \frac{P^2}{2m_B(D)} \qquad (41)$$

and

$$\mathcal{E}_{1,0}(P) = \frac{1}{2}\big[\mathcal{E}_{00}^{(b)}(B, D) + \mathcal{E}_{01}^{(b)}(B, D)\big]$$

$$+ \frac{1}{2}\left(\frac{P^2}{2M_{00}(B, D)} + \frac{P^2}{2M_{01}(B, D)}\right)$$

$$= -\mathcal{E}_B^{(b)}(D) + \frac{P^2}{2m_B(D)}, \qquad (42)$$

where the binding energy $\mathcal{E}_B^{(b)}(D)$ and the effective magnetic mass $m_B(D)$ of a magnetoexciton with spatially separated electrons and holes in the $\alpha$-$\mathcal{T}_3$ double layer are, for case 1,

$$\mathcal{E}_B^{(b)}(D) = -\frac{1}{4}\big[\mathcal{E}_{00}^{(b)}(B, D) + 2\mathcal{E}_{01}^{(b)}(B, D) + \mathcal{E}_{10}^{(b)}(B, D)\big],$$

$$\frac{1}{m_B(D)} = \frac{1}{4}\Big[\frac{1}{M_{00}(B, D)} + \frac{2}{M_{01}(B, D)} + \frac{1}{M_{10}(B, D)}\Big], \qquad (43)$$

and, for case 2,

$$\mathcal{E}_B^{(b)}(D) = -\frac{1}{2}\big[\mathcal{E}_{00}^{(b)}(B, D) + \mathcal{E}_{01}^{(b)}(B, D)\big],$$

$$\frac{1}{m_B(D)} = \frac{1}{2}\Big(\frac{1}{M_{00}(B, D)} + \frac{1}{M_{01}(B, D)}\Big), \qquad (44)$$

where the constants $\mathcal{E}_{00}^{(b)}(B, D)$, $\mathcal{E}_{01}^{(b)}(B, D)$, $\mathcal{E}_{10}^{(b)}(B, D)$, $M_{00}(B, D)$, $M_{01}(B, D)$, and $M_{10}(B, D)$, depending on

magnetic field $B$ and the interlayer separation $D$, are defined by [26]

$$\mathcal{E}_{00}^{(b)}(B,D) = -\mathcal{E}_0 \exp\left[\frac{D^2}{2r_B^2}\right]\text{erfc}\left[\frac{D}{\sqrt{2}r_B}\right],$$

$$\mathcal{E}_{01}^{(b)}(B,D) = -\mathcal{E}_0\left\{\left(\frac{1}{2} - \frac{D^2}{2r_B^2}\right)\exp\left[\frac{D^2}{2r_B^2}\right]\text{erfc}\left[\frac{D}{\sqrt{2}r_B}\right] + \frac{D}{\sqrt{2\pi}r_B}\right\},$$

$$\mathcal{E}_{10}^{(b)}(B,D) = -\mathcal{E}_0\left\{\left(\frac{3}{4} + \frac{D^2}{2r_B^2} + \frac{D^4}{4r_B^4}\right)\exp\left[\frac{D^2}{2r_B^2}\right]\text{erfc}\left[\frac{D}{\sqrt{2}r_B}\right] - \frac{D}{2\sqrt{2\pi}r_B} - \left(\frac{D}{\sqrt{2}r_B}\right)^3\frac{1}{\sqrt{\pi}}\right\},$$

$$M_{00}(B,D) = M_0\left\{\left(1 + \frac{D^2}{r_B^2}\right)\exp\left[\frac{D^2}{2r_B^2}\right]\text{erfc}\left[\frac{D}{\sqrt{2}r_B}\right] - \sqrt{\frac{2}{\pi}}\frac{D}{r_B}\right\}^{-1},$$

$$M_{01}(B,D) = M_0\left\{\left(3 + \frac{D^2}{r_B^2}\right)\frac{D}{\sqrt{2\pi}r_B} - \left(\frac{1}{2} + 2\frac{D^2}{r_B^2} + \frac{D^4}{2r_B^4}\right)\exp\left[\frac{D^2}{2r_B^2}\right]\text{erfc}\left[\frac{D}{\sqrt{2}r_B}\right]\right\}^{-1},$$

$$M_{10}(B,D) = M_0\left\{\frac{1}{4}\left(7 + 25\frac{D^2}{r_B^2} + 11\frac{D^4}{r_B^4} + \frac{D^6}{r_B^6}\right)\exp\left[\frac{D^2}{2r_B^2}\right]\text{erfc}\left[\frac{D}{\sqrt{2}r_B}\right] - \left(\frac{17}{2} + 5\frac{D^2}{r_B^2} + \frac{D^4}{2r_B^4}\right)\frac{D}{\sqrt{2\pi}r_B}\right\}^{-1},$$

(45)

where the constants $\mathcal{E}_0$ and $M_0$ and function $\text{erfc}(z)$ are given by [26]

$$\mathcal{E}_0 = \left\langle\left\langle 00\mathbf{P}\left|\frac{e^2}{\epsilon|\mathbf{r}|}\right|00\mathbf{P}\right\rangle\right\rangle_{\mathbf{P}=0} = \frac{ke^2}{\epsilon r_B}\sqrt{\frac{\pi}{2}},$$

$$M_0 = -\left[2\left(\left\langle\left\langle 00\mathbf{P}\left|\frac{e^2}{\epsilon|\mathbf{r}|}\right|00\mathbf{P}\right\rangle\right\rangle - \mathcal{E}_0\right)\right]^{-1}P^2 = \frac{2^{3/2}\epsilon\hbar^2}{\sqrt{\pi}ke^2r_B},$$

$$\text{erfc}(z) = \frac{2}{\sqrt{\pi}}\int_z^\infty \exp(-t^2)dt. \quad (46)$$

For both cases 1 and 2, for large interlayer separation $D \gg r_B$, the asymptotic values for the binding energy $\mathcal{E}_B^{(b)}(D)$ and the effective magnetic mass $m_B(D)$ of the dipolar magnetoexciton in the $\alpha\text{-}\mathcal{T}_3$ double layer are the same and are given by

$$\mathcal{E}_B^{(b)}(B,D) = \frac{ke^2}{\epsilon D}, \quad m_B(D) = \frac{\epsilon D^3 B^2}{k}. \quad (47)$$

Measuring energy from the binding energy of the magnetoexciton, the dispersion relation $\varepsilon_k(P)$ for an isolated dipolar magnetoexciton is a quadratic function at small magnetic momentum $P \ll \hbar/r_B$ and $P \ll \hbar D/r_B^2$:

$$\varepsilon_k(\mathbf{P}) = \frac{P^2}{2m_{Bk}}, \quad (48)$$

where $m_{Bk}$, the effective magnetic mass, is dependent on $B$ and the separation $D$ between electron and hole layers as well as the quantum number $k$ [$k = (n_e, n_h)$ are magnetoexcitonic quantum numbers].

The squared 2D radius of a magnetoexciton for case 1 can be defined as

$$r_{1,1}^2(P=0) = \langle 1,1,\mathbf{P}|r^2|1,1,\mathbf{P}\rangle_{\mathbf{P}=0}$$
$$= \frac{1}{4}(l_{00}^2 + 2l_{01}^2 + l_{10}^2) = 4r_B^2, \quad r_{1,1} = 2r_B, \quad (49)$$

and for case 2 it can be defined as

$$r_{1,0}^2(P=0) = \langle 1,0,\mathbf{P}|r^2|1,0,\mathbf{P}\rangle_{\mathbf{P}=0}$$
$$= \frac{1}{2}(l_{00}^2 + l_{01}^2) = 3r_B^2, \quad r_{1,0} = \sqrt{3}r_B, \quad (50)$$

where $l_{\tilde{n}m}^2 = \langle\langle\tilde{n}m\mathbf{P}|\hat{r}^2|\tilde{n}m\mathbf{P}\rangle\rangle_{\mathbf{P}=0}$ and ($l_{00}^2 = 2r_B^2$, $l_{01}^2 = 4r_B^2$, $l_{10}^2 = 6r_B^2$) [26].

## V. SUPERFLUIDITY OF DIPOLAR MAGNETOEXCITONS IN AN $\alpha\text{-}\mathcal{T}_3$ DOUBLE LAYER

Dipolar magnetoexcitons have electrical dipole moments, produced by the interlayer separation $D$. We assume that dipolar magnetoexcitons repel each other like parallel dipoles. The latter assumption is reasonable when $D$ is larger than the mean separation between an electron and hole parallel to the $\alpha\text{-}\mathcal{T}_3$ layers $D \gg (\langle r^2\rangle)^{1/2}$.

Since electrons on an $\alpha\text{-}\mathcal{T}_3$ monolayer can be located in two valleys, there are four types of dipolar magnetoexcitons in an $\alpha\text{-}\mathcal{T}_3$ double layer. Since all these types of dipolar magnetoexcitons have identical envelope wave functions and energies, it is reasonable to assume that a dipolar magnetoexciton is located in only one valley. We use $n_0 = n/(4s)$ as the density of magnetoexcitons in one valley, where $n$ is the total density of magnetoexcitons and $s$ is the spin degeneracy ($s = 4$ for magnetoexcitons in an $\alpha\text{-}\mathcal{T}_3$ double layer).

We shall treat a dilute 2D magnetoexciton system in the $\alpha\text{-}\mathcal{T}_3$ double layer as a weakly interacting Bose gas by applying the procedure described in Ref. [9]. Two dipolar magnetoexcitons in a dilute structure repel each other with the potential energy of the pair magnetoexciton-magnetoexciton interaction, written as $U(R) = ke^2D^2/(\epsilon R^3)$, where $R$ is the distance between magnetoexciton dipoles parallel to the $\alpha\text{-}\mathcal{T}_3$ layers. For the weakly interacting Bose gas of 2D dipolar magnetoexcitons [when $na^2(B) \ll 1$, where $a(B)$ is the in-plane radius of a dipolar magnetoexciton defined for cases 1 and 2 in Eqs. (49) and (50), respectively] the summation of ladder diagrams is valid [48]. The chemical potential $\mu$,
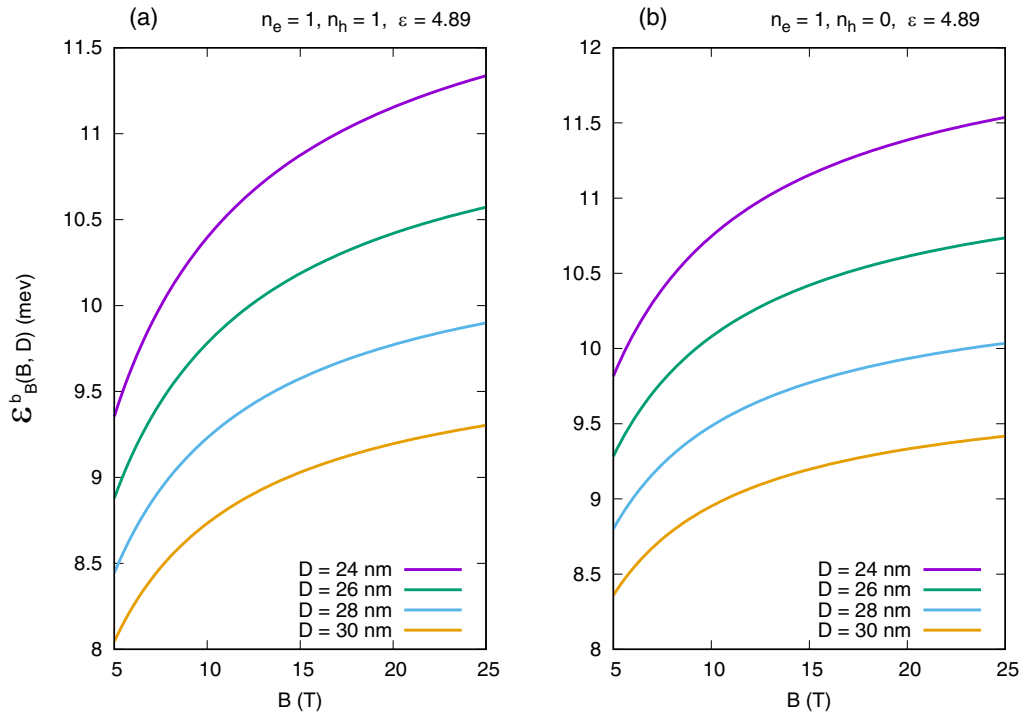
FIG. 3. The magnetoexciton binding energy $\mathcal{E}_B^b(B, D)$ as a function of magnetic field $B$ for chosen interlayer separations $D$ for (a) case 1 and (b) case 2.

corresponding to the summation of the ladder diagrams, can be written as [9]

$$\mu = \frac{\kappa^2}{2m_B} = \frac{\pi \hbar^2 n}{sm_B \ln \left[ s\hbar^4 \epsilon^2 / (2\pi n m_B^2 k^2 e^4 D^4) \right]}, \quad (51)$$

where $s = 4$ is the spin degeneracy factor.

The spectrum of collective excitations, obtained from the ladder approximation, at low magnetic momenta corresponds to the sound spectrum of collective excitations $\varepsilon(P) = c_s P$ with the sound velocity $c_s = \sqrt{\mu/m_B}$, where $\mu$ is defined by Eq. (51). Since magnetoexcitons have a sound spectrum for collective excitations at small magnetic momenta $P$ due to dipole-dipole repulsion, the magnetoexcitonic superfluidity is possible at low temperatures $T$ in $\alpha$-$\mathcal{T}_3$ double layers because the sound spectrum satisfies the Landau criterion for superfluidity [48,49].

The magnetoexcitons constructed from spatially separated electrons and holes in $\alpha$-$\mathcal{T}_3$ double layers with large interlayer separation $D \gg r_B$ form a weakly interacting 2D gas of bosons with dipole-dipole pair repulsion. Consequently, the superfluid-normal phase change in this system is the Kosterlitz-Thouless transition [50]. The temperature $T_c$ of this

conversion to the superfluid state in a 2D magnetoexciton system is determined by the equation

$$T_c = \frac{\pi \hbar^2 n_s(T_c)}{2 k_B m_B}, \quad (52)$$

where $n_s(T)$ is the superfluid density of the magnetoexciton system as a function of temperature $T$, magnetic field $B$, and interlayer separation $D$ and $k_B$ is the Boltzmann constant. The function $n_s(T)$ in Eq. (52) can be determined from the relation $n_s = n/(4s) - n_n$, where $n$ is the total density and $n_n$ is the normal component density. Following the procedure described in Ref. [9], we have for the superfluid density

$$n_s = \frac{n}{4s} - n_n = \frac{n}{4s} - \frac{3\zeta(3)}{2\pi \hbar^2} \frac{k_B^3 T^3}{c_s^4 m_B}. \quad (53)$$

In a 2D system, superfluidity of magnetoexcitons appears below the Kosterlitz-Thouless transition temperature [Eq. (52)], where only coupled vortices are present [50]. Using Eq. (53) for the density $n_s$ of the superfluid component, we obtain an equation for the Kosterlitz-Thouless transition temperature $T_c$. Its solution is

$$T_c = \left\{ \left[ 1 + \sqrt{\frac{32}{27} \left( \frac{sm_B k_B T_c^0}{\pi \hbar^2 n} \right)^3 + 1} \right]^{1/3} - \left[ \sqrt{\frac{32}{27} \left( \frac{sm_B k_B T_c^0}{\pi \hbar^2 n} \right)^3 + 1} - 1 \right]^{1/3} \right\} \frac{T_c^0}{2^{1/3}}. \quad (54)$$

Here $T_c^0$ is the temperature at which the superfluid density vanishes in the mean-field approximation [i.e., $n_s(T_c^0) = 0$],

$$T_c^0 = \frac{1}{k_B} \left( \frac{\pi \hbar^2 n c_s^4 m_B}{6s\zeta(3)} \right)^{1/3}. \quad (55)$$
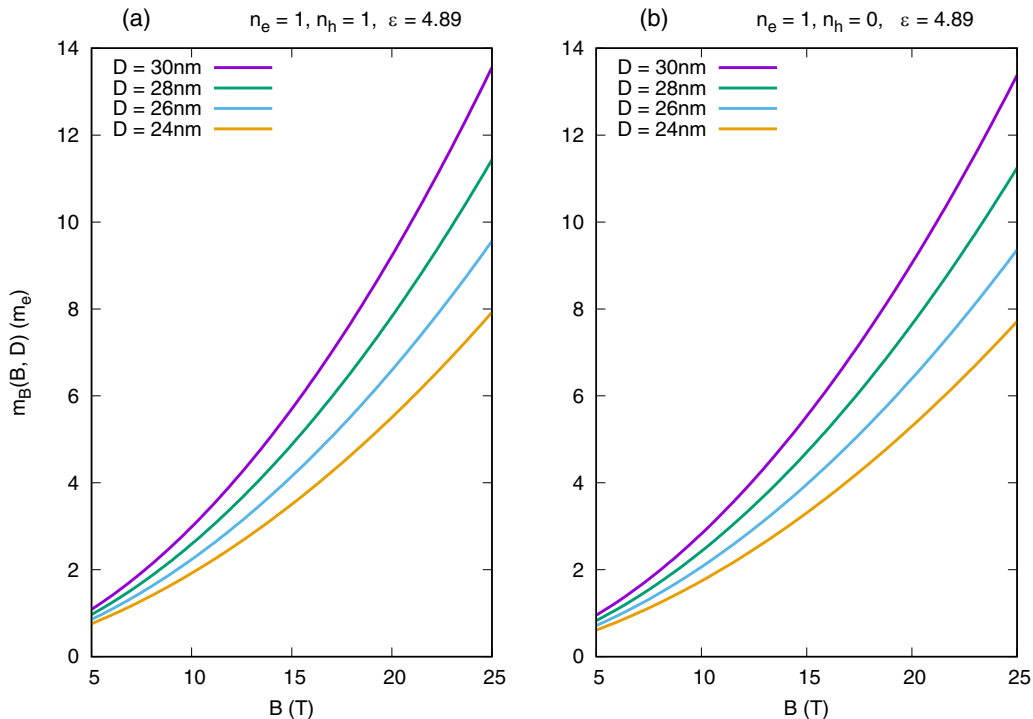
FIG. 4. The effective magnetic mass $m_B(B, D)$ of a magnetoexciton as a function of magnetic field $B$ for chosen interlayer separation $D$ for (a) case 1 and (b) case 2.

In Fig. 3, we present results showing the dependence of the magnetoexciton binding energy $\mathcal{E}_B^b(B, D)$ on the magnetic field $B$ for chosen interlayer separation $D$ in cases 1 and 2. According to Fig. 3, $\mathcal{E}_B^b(B, D)$ is increased as $B$ is increased, and $D$ is decreased. For the same parameters $\mathcal{E}_B^b(B, D)$ is slightly larger for case 2 than case 1.

Figure 4 presents our results for the dependence of the effective magnetic mass $m_B(B, D)$ of a magnetoexciton on the magnetic field $B$ for chosen interlayer separation $D$ for cases 1 and 2. According to Fig. 4, $m_B(B, D)$ increases as $B$ is increased and $D$ is increased. For the same parameters, $m_B(B, D)$ is slightly larger for case 1 compared with case 2.

In Fig. 5, we display our results for the Kosterlitz-Thouless transition temperature $T_c(n, B, D)$ versus the magnetic field $B$ for various interlayer separations at fixed magnetoexciton concentration $n$ for cases 1 and 2. According to Fig. 5, $T_c(n, B, D)$ decreases as $B$ is increased and $D$ is increased. For the same parameters, $T_c(n, B, D)$ is slightly larger for case 2 compared with case 1.

We plot in Fig. 6 the functional dependence of the Kosterlitz-Thouless transition temperature $T_c(n, B, D)$ on the magnetoexciton concentration $n$ for several chosen magnetic fields $B$ and fixed interlayer separation $D$ in both cases 1 and 2. We deduce from Fig. 6 that $T_c(n, B, D)$ increases as $n$ is increased but decreases as $B$ is increased. Additionally, we conclude that for the same values of the parameters, $T_c(n, B, D)$ is slightly larger for case 2 than case 1.

Based on Figs. 3, 5, and 6, one can conclude that case 2 is slightly preferable to case 1 for observing dipolar magnetoexcitons and their superfluidity in the $\alpha$-$\mathcal{T}_3$ double layer since case 2 corresponds to slightly larger magnetoexciton binding energy $\mathcal{E}_B^b(B, D)$ and Kosterlitz-Thouless transition

temperature $T_c(n, B, D)$ than case 1 for the same described parameters.

If the $\alpha$-$\mathcal{T}_3$ double layer is surrounded by air, a lower effective dielectric constant $\epsilon$ will result in higher magnetoexciton binding energy $\mathcal{E}_B^{(b)}(B, D)$ and lower effective magnetic mass of a magnetoexciton $m_B(D)$ at the same magnetic field strength $B$ and layer separation $D$ according to Eqs. (46) and (47). Lower $m_B(D)$ will correspond to higher Kosterlitz-Thouless transition temperature $T_c(n, B, D)$, which follows from Eqs. (54) and (55). Therefore, embedding the $\alpha$-$\mathcal{T}_3$ double layer in air, implying a lower effective dielectric constant $\epsilon$, will lead to a higher Kosterlitz-Thouless transition temperature $T_c(n, B, D)$ for the same $B$ and $D$. However, if the pair of $\alpha$-$\mathcal{T}_3$ layers is separated by a dielectric, the lifetime of dipolar excitons is expected to be higher than for the case when these layers are separated by air. The reason is that due to the tunneling of electrons and holes, the electron-hole recombination associated with different $\alpha$-$\mathcal{T}_3$ layers is suppressed by the dielectric barrier that separates the layers. Therefore, the dipolar excitons with a dielectric medium between the layers can have a very long lifetime, and therefore, they can be treated as metastable particles described by quasiequilibrium statistics.

## VI. CONCLUSIONS

In this paper, we have proposed the occurrence of BEC and superfluidity of dipolar magnetoexcitons in $\alpha$-$\mathcal{T}_3$ double layers in a strong uniform perpendicular magnetic field. The low-energy Hamiltonian for a single $\alpha$-$\mathcal{T}_3$ layer was obtained by including additional hopping terms in a single-layer graphene Dirac Hamiltonian. We have obtained the solution
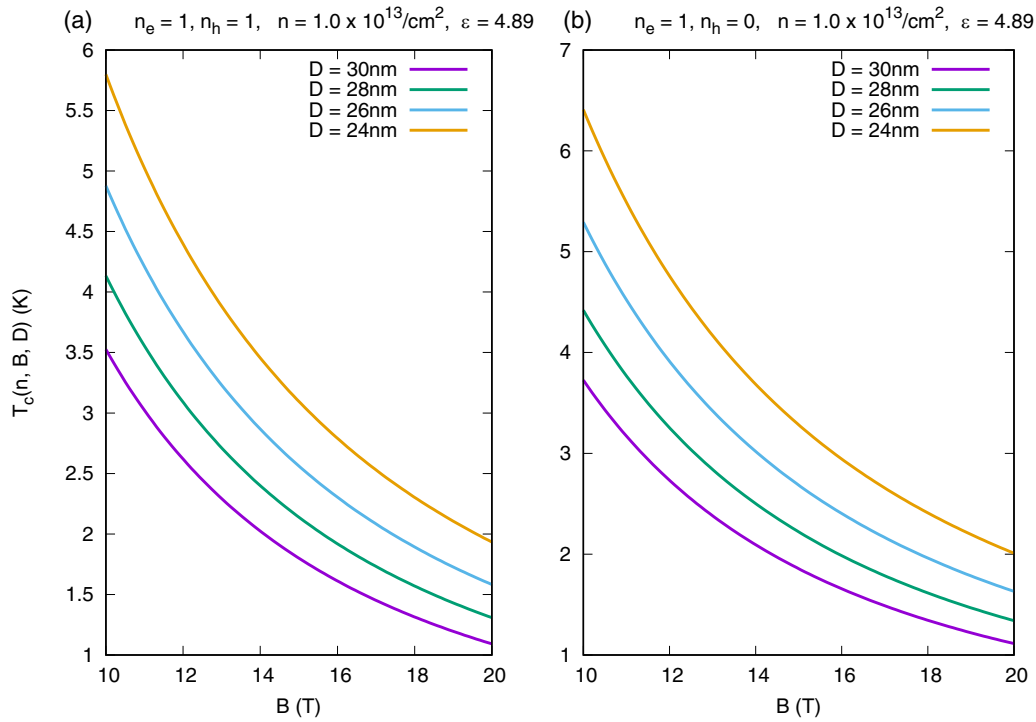
FIG. 5. The Kosterlitz-Thouless transition temperature $T_c(n, B, D)$ versus magnetic field $B$ for chosen interlayer separations $D$ at the fixed magnetoexciton concentration $n$ for (a) case 1 and (b) case 2.

of a two-body problem for an electron and a hole for the model Hamiltonian for the $\alpha\text{-}\mathcal{T}_3$ double layer in a magnetic field. We have calculated the binding energy, effective mass, spectrum of collective excitations, superfluid density, and temperature of the Kosterlitz-Thouless phase transition to the

superfluid state for dipolar magnetoexcitons in the $\alpha\text{-}\mathcal{T}_3$ double layer. We have demonstrated that at fixed exciton density, the Kosterlitz-Thouless temperature for superfluidity of dipolar magnetoexcitons is decreased as a function of magnetic field. Our results show that $T_c$ increases as a function of
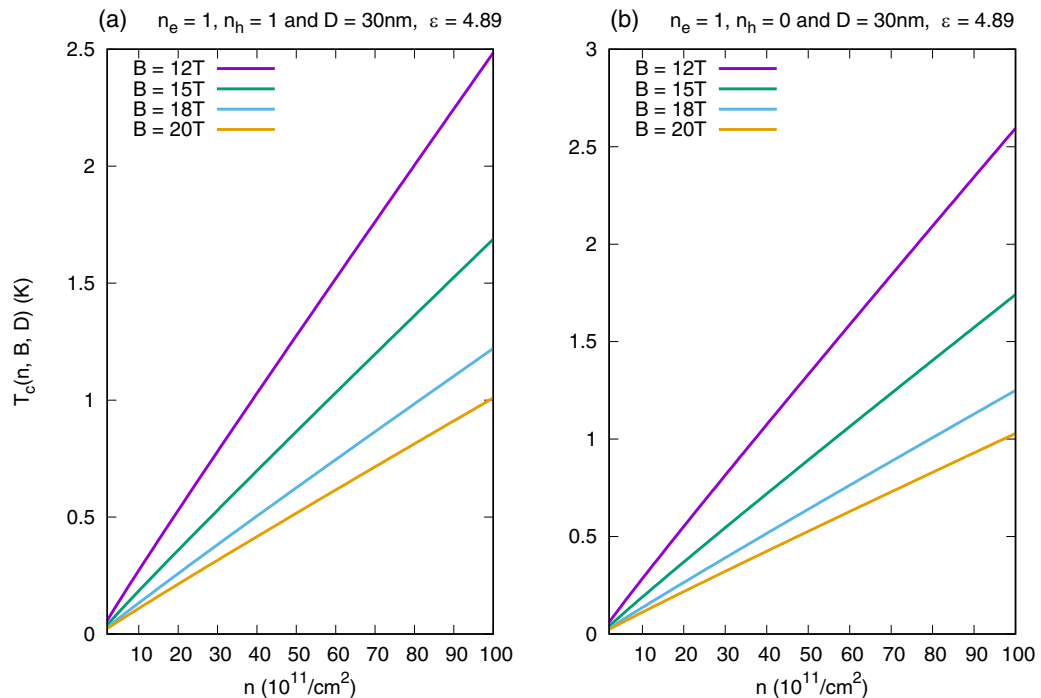


FIG. 6. The Kosterlitz-Thouless transition temperature $T_c(n, B, D)$ as a function of the magnetoexciton concentration $n$ for various magnetic fields $B$ and fixed interlayer separation $D$ for (a) case 1 and (b) case 2.

the density $n$ and decreases as a function of the magnetic field $B$ and the interlayer separation $D$. We have demonstrated that case 2 (in which the dipolar magnetoexciton is formed by an electron in Landau level 1 and a hole in Landau level 0) is slightly preferable to case 1 (in which the dipolar magnetoexciton is formed by an electron in Landau level 1 and a hole in Landau level $-1$) to observe the dipolar magnetoexcitons and their superfluidity in $\alpha$-$\mathcal{T}_3$ double layers. The reason is that case 2 corresponds to a slightly larger magnetoexciton binding energy and Kosterlitz-Thouless transition temperature than case 1 for the same chosen parameters.

The superfluid state for $T < T_c$ can lead to the existence of persistent dissipationless superconducting oppositely directed electric currents in each $\alpha$-$\mathcal{T}_3$ layer, forming a double layer. According to the reported results of our calculations, while the external magnetic field has the desired effect of increasing the magnetoexciton binding energy, we have found that the Kosterlitz-Thouless transition temperature to the superfluid phase increases as the magnetic field is decreased. This suggests that one may employ a dipolar magnetoexciton system in a double-layer to engineer a switch, where transport properties of magnetoexcitons can be controlled by an external magnetic field. Varying a quantizing magnetic field can result in a phase transition between the superfluid and normal phases, thereby changing the transport properties of magnetoexcitons in a substantial way.

Our approach to study the superfluidity of dipolar magnetoexcitons in double layers can be generalized and applied to other two-dimensional materials. In particular, we are interested in investigating a method of controlling the superfluidity of dipolar magnetoexcitons in TMDC double layers by an external magnetic field in future work. TMDC double layers seem to be a promising system to study electron-hole superfluity due to relatively high $T_c$ measured without magnetic field in recent experiments (around 100 K) [21,51].

[1] Yu. E. Lozovik and V. I. Yudson, Phys. JETP Lett. **22**, 26 (1975); Sov. Phys. JETP **44**, 389 (1976).

[2] D. W. Snoke, Science **298**, 1368 (2002).

[3] L. V. Butov, J. Phys.: Condens. Matter **16**, R1577 (2004).

[4] J. P. Eisenstein and A. H. MacDonald, Nature (London) **432**, 691 (2004).

[5] D. W. Snoke, in *Quantum Gases: Finite Temperature and Non-equilibrium Dynamics*, edited by N. P. Proukakis, S. A. Gardiner, M. J. Davis, and M. H. Szymanska, Cold Atom Series Vol. 1 (Imperial College Press, London, 2013), p. 419.

[6] S. Saberi-Pouya, S. Conti, A. Perali, A. F. Croxall, A. R. Hamilton, F. M. Peeters, and D. Neilson, Phys. Rev. B **101**, 140501(R) (2020).

[7] P. López Ríos, A. Perali, R. J. Needs, and D. Neilson, Phys. Rev. Lett. **120**, 177701 (2018).

[8] A. Perali, D. Neilson, and A. R. Hamilton, Phys. Rev. Lett. **110**, 146803 (2013).

[9] O. L. Berman, Yu. E. Lozovik, and G. Gumbs, Phys. Rev. B **77**, 155433 (2008).

[10] Yu. E. Lozovik and A. A. Sokolik, JETP Lett. **87**, 55 (2008); Phys. Lett. A **374**, 326 (2009).

[11] R. Bistritzer and A. H. MacDonald, Phys. Rev. Lett. **101**, 256406 (2008).

[12] O. L. Berman, R. Ya. Kezerashvili, and K. Ziegler, Phys. Rev. B **85**, 035418 (2012).

[13] M. M. Fogler, L. V. Butov, and K. S. Novoselov, Nat. Commun. **5**, 4555 (2014).

[14] F.-C. Wu, F. Xue, and A. H. MacDonald, Phys. Rev. B **92**, 165121 (2015).

[15] O. L. Berman and R. Ya. Kezerashvili, Phys. Rev. B **93**, 245410 (2016).

[16] O. L. Berman and R. Ya. Kezerashvili, Phys. Rev. B **96**, 094502 (2017).

[17] S. Conti, M. Van Donck, A. Perali, F. M. Peeters, and D. Neilson, Phys. Rev. B **101**, 220504(R) (2020).

[18] O. L. Berman, G. Gumbs, and R. Ya. Kezerashvili, Phys. Rev. B **96**, 014505 (2017).

[19] S. Saberi-Pouya, M. Zarenia, A. Perali, T. Vazifehshenas, and F. M. Peeters, Phys. Rev. B **97**, 174503 (2018).

[20] Y. Mazuz-Harpaz, K. Cohen, M. Leveson, K. West, L. Pfeiffer, M. Khodas, and R. Rapaport, Proc. Natl. Acad. Sci. U.S.A. **116**, 18328 (2019).

[21] Z. Wang, D. A. Rhodes, K. Watanabe, T. Taniguchi, J. C. Hone, J. Shan, and K. Fai Mak, Nature (London) **574**, 76 (2019).

[22] I. V. Lerner and Yu. E. Lozovik, Sov. Phys. JETP **51**, 588 (1980); **53**, 763 (1981); A. B. Dzyubenko and Yu. E. Lozovik, J. Phys. A **24**, 415 (1991).

[23] D. Paquet, T. M. Rice, and K. Ueda, Phys. Rev. B **32**, 5208 (1985).

[24] C. Kallin and B. I. Halperin, Phys. Rev. B **30**, 5655 (1984); **31**, 3635 (1985).

[25] D. Yoshioka and A. H. MacDonald, J. Phys. Soc. Jpn. **59**, 4211 (1990).

[26] Yu. E. Lozovik and A. M. Ruvinsky, Phys. Lett. A **227**, 271 (1997); J. Exp. Theor. Phys. **85**, 979 (1997).

[27] M. A. Olivares-Robles and S. E. Ulloa, Phys. Rev. B **64**, 115302 (2001).

[28] S. A. Moskalenko, M. A. Liberman, D. W. Snoke, and V. V. Botan, Phys. Rev. B **66**, 245316 (2002).

[29] A. Spiridonova, Phys. Lett. A **384**, 126850 (2020).

[30] A. Raoux, M. Morigi, J.-N. Fuchs, F. Piéchon, and G. Montambaux, Phys. Rev. Lett. **112**, 026402 (2014).

[31] B. Sutherland, Phys. Rev. B **34**, 5208 (1986).

[32] E. Illes, J. P. Carbotte, and E. J. Nicol, Phys. Rev. B **92**, 245410 (2015).

[33] SK Firoz Islam and P. Dutta, Phys. Rev. B **96**, 045418 (2017).

[34] E. Illes and E. J. Nicol, Phys. Rev. B **94**, 125435 (2016).

[35] B. Dey and T. K. Ghosh, Phys. Rev. B **98**, 075422 (2018).

[36] B. Dey and T. K. Ghosh, Phys. Rev. B **99**, 205429 (2019).

[37] T. Biswas and T. K. Ghosh, J. Phys.: Condens. Matter **30**, 075301 (2018).

[38] A. D. Kovacs, G. David, B. Dora, and J. Cserti, Phys. Rev. B **95**, 035414 (2017).

[39] T. Biswas and T. K. Ghosh, J. Phys.: Condens. Matter **28**, 495302 (2016).

[40] D. O. Oriekhov and V. P. Gusynin, Phys. Rev. B **101**, 235162 (2020).

[41] D. Huang, A. Iurov, H.-Y. Xu, Y.-C. Lai, and G. Gumbs, Phys. Rev. B **99**, 245412 (2019).

[42] Y. Li, S. Kita, P. Munoz, O. Reshef, D. I. Vulis, M. Yin, M. Loncar, and E. Mazur, Nat. Photonics **9**, 738 (2015).

[43] H.-Y. Xu, L. Huang, D. H. Huang, and Y.-C. Lai, Phys. Rev. B **96**, 045412 (2017).

[44] D. Leykam, A. Andreanov, and S. Flach, Adv. Phys.: X **3**, 677 (2018).

[45] M. Sherafati and S. Satpathy, Phys. Rev. B **84**, 125416 (2011).

[46] A. Iyengar, J. Wang, H. A. Fertig, and L. Brey, Phys. Rev. B **75**, 125430 (2007).

[47] Y. Cai, L. Zhang, Q. Zeng, L. Cheng, and Y. Xu, Solid State Commun. **141**, 262 (2007).

[48] A. A. Abrikosov, L. P. Gorkov, and I. E. Dzyaloshinski, *Methods of Quantum Field Theory in Statistical Physics* (Prentice-Hall, Englewood Cliffs, NJ, 1963).

[49] A. Griffin, *Excitations in a Bose-Condensed Liquid* (Cambridge University Press, Cambridge, 1993).

[50] J. M. Kosterlitz and D. J. Thouless, J. Phys. C **6**, 1181 (1973); D. R. Nelson and J. M. Kosterlitz, Phys. Rev. Lett. **39**, 1201 (1977).

[51] A. Chaves and D. Neilson, Nature (London) **574**, 40 (2019).